IL NUOVO CIMENTO **45 C** (2022) 59
DOI 10.1393/ncc/i2022-22059-x

Colloquia: IWM-EC 2021

Microscopic description of 2α-decay in ^{212}Po and ^{224}Ra isotopes

F. Mercier(1)(*), J. Zhao(2), J.-P. Ebran(3)(4), E. Khan(1),
T. Nikšić(5) and D. Vretenar(5)

(1) *IJCLab, Université Paris-Saclay, CNRS/IN2P3 - 91405 Orsay Cedex, France*
(2) *Center for Circuits and Systems, Peng Cheng Laboratory - Shenzhen 518055, China*
(3) *CEA,DAM,DIF - F-91297 Arpajon, France*
(4) *Université Paris-Saclay, CEA, Laboratoire Matière en Conditions Extrêmes - 91680, Bruyères-le-Châtel, France*
(5) *Physics Department, Faculty of Science, University of Zagreb - 10000 Zagreb, Croatia*

received 12 May 2022

Summary. — Half-lives calculations for α decay of ^{212}Po and ^{224}Ra are performed using microscopic self-consistent framework. Calculations are performed using the covariant energy density functional theory within Hartree-Bogoliubov approximation, where a separable pairing interaction of finite range is used. The potential energy surface is computed as a function of quadrupole, octupole and hexadecupole collective coordinates and the determination of the dynamical least-action path is performed using the cranking adiabatic time-dependent Hartree Bogoliubov approximation. The predicted half-lives for α decay of ^{212}Po and ^{224}Ra are in good agreement with experimental values. In addition, a new decay mode consisting of symmetric, back to back, 2α emission is predicted with half-lives of the order of those observed for cluster emission.

Introduction

The study of radioactive decays, initiated more than a hundred years ago with the observation of α decay, remains a particularly difficult problem in physics [1]. In views of the various decay modes already known such as α decay or fission process but also more exotic ones such as cluster decays [2] and two-proton radioactivity [3,4], it remains highly probable that (many) other decay modes are still to be identified. In particular, few semi-microscopic approaches have already indicated the possible existence of a new 2α decay considered as a ^{8}Be-like mode [5,6]. The latter, very unstable, decays into two

(*) E-mail: `florian.mercier@ijclab.in2p3.fr`

α particles with $T_{1/2} \simeq 10^{-16}$ sec. These models predict half-lives of $T_{1/2} \simeq 10^{33}$ years or more for 2α decay, making the experimental detection very unlikely.

The already experimentally known processes of alpha, cluster and fission decay are quite well understood using semi-microscopic methods [7,8]. Fully-microscopical methods also gave quantitative results in the description of cluster decay within the framework of (non-relativistic Gogny) energy density functional (EDF) and Hartree-Fock Bogoliubov (HFB) approximation [9, 10]. The framework of covariant EDF used in the present work has already been widely used to describe nuclear structure phenomena [11], cluster states [12, 13], spontaneous and induced fission [14-18], and α-decay [19-21].

More recently, the study of ref. [19] showed the possibility to obtain quantitative half-lives results of ^{108}Xe $\rightarrow$ ^{104}Te $\rightarrow$ ^{100}Sn α-decay chain. This study used the relativistic point-coupling DD-PC1 interaction as well as a separable pairing interaction. The potential energy surface (PES) was computed using axially-symmetric deformations (quadrupolar and octupolar). The lifetime computation was performed using cranking perturbative adiabatic time-dependent Hartree Bogoliubov (cATDHB) approximation. The present study aims to describe the α decay for higher mass nuclei, namely ^{212}Po and ^{224}Ra as well as possible 2α-decays in the same region. This last mode would correspond to the emission of two α particles emitted back to back in a symmetric way. Thus, this mode differs from a ^{8}Be emission, which would also lead to 2α decay, and in particular significantly reduces the predicted half-lives.

Theoretical framework

A detailed description of the relativistic Hartree-Bogoliubov (RHB) self-consistent model can be found in refs. [11,22,23]. This framework is used here to perform constraint calculations in a 3-dimensional collective space $(\beta_{20}, \beta_{30}, \beta_{40})$ to compute a 3-dimensional potential energy surface. In the case of 2α decay, the reflection symmetry of the system allows for a 2-dimensional study in the (β_{20}, β_{40}) coordinates space. The L path is determined by minimizing the action integral [24, 25]

$$S(L) = \int_{s_{\mathrm{in}}}^{s_{\mathrm{out}}} \frac{1}{\hbar} \sqrt{2\mathcal{M}_{\mathrm{eff}}(s)\,[V_{\mathrm{eff}}(s) - E_0]}\mathrm{d}s, \tag{1}$$

where $\mathcal{M}_{\mathrm{eff}}(s)$ and $V_{\mathrm{eff}}(s)$ are the effective collective inertia and potential, respectively. E_0 is the collective ground-state energy, and the integration limits correspond to the classical inner (s_{in}) and outer (s_{out}) turning points, defined by $V_{\mathrm{eff}}(s) = E_0$. The inner point is chosen as the RHB configuration minimizing the energy of the system. Then, the path is divided in two steps. A first going from the inner point to the scission point defined as the point where the integrated density distribution of the cluster is equal to the mass of the α particle (or 2α particles). Then, beyond the scission point, a fully microscopical calculation is not necessary and the configuration with two (or three) well separated fragments can be approximated by the classical expression for two uniformly charged spheres:

$$V_{\mathrm{eff}}(\beta_3) = e^2 \frac{Z_1 Z_2}{R} - Q, \tag{2}$$

where R denotes the distance between the centres of mass of the fragments, and the second term is the experimental Q value. The relation between R and the octupole moment q_{30} is approximated following eqs. (9) and (10) of ref. [9] $q_{30} = f_3 R^3$, with $f_3 = \frac{A_1 A_2}{A} \frac{(A_1 - A_2)}{A}$, and $\beta_{30} = 4\pi q_{30}/3AR^3$. The corresponding effective mass follows the result of [9]. The α-decay half-life is calculated as $T_{1/2} = \ln 2/(nP)$, where n is the number of assaults on the potential barrier per unit time [26-29], and P is the barrier penetration probability in the WKB approximation

$$P = \frac{1}{1 + \exp[2S(L)]}. \tag{3}$$

We choose $E_0 = 1\,\mathrm{MeV}$ in eq. (1) for the value of the collective ground state energy. The corresponding value for the vibrational frequency $\hbar\omega = 1\,\mathrm{MeV}$ is $n = 10^{20.38}\,\mathrm{s}^{-1}$ [9, 30]. The effective inertia in eq. (1) is computed from the multidimensional collective inertia tensor $\mathcal{M}$, see [24, 26-29] for more details. The collective inertia tensor is calculated in the perturbative cranking approximation (see ref. [14] and references cited therein). The effective collective potential $V_{\rm eff}$ is calculated by subtracting the vibrational zero-point energy (ZPE) from the total RHB deformation energy. The zero-point energy is computed using the Gaussian overlap approximation, see [28, 29, 31, 32].

In the present work, the RHB equations are solved using an expansion of the nucleons spinors in an axially harmonic oscillator basis with $N_f = 20$ ($N_g = N_f + 1$) major oscillator for the large (small) component of the Dirac spinor. The technical details of the solution of the constrained RHB equations can be found in refs. [14,33]. The obtained RHB states are then used as an input for the calculation of both the collective inertia and zero-point energy. DD-PC1 [34] relativistic functional is used here in the particle-hole channel, and a separable pairing interaction of finite-range [35]. This interaction was originally adjusted on the results of the D1S parametrization of the Gogny force results to reproduce the pairing gap in nuclear matter. Here, however, neutron and proton pairing strengths are adjusted to reproduce empirical pairing gaps of the ^{224}Ra isotope as already mentioned in a previous study [36]. The difference between old and new values of the pairing strengths are of the order of 10% both in neutron and proton channels.

Application to α decay

As a benchmark and to test the model in the heavy nuclei region, the case of the well known α-emitter ^{212}Po is depicted. Figure 1 displays the deformation energy surface of ^{212}Po in the (β_{20}, β_{30}) plane for several values of the hexadecupole deformation β_{40}. One notices that, for deformations $\beta_{40} \geq 0.5$ and $(\beta_{20}, \beta_{30}) \simeq (0.15, 0.3)$, a pronounced minimum develops on the deformation energy surface at approximately 25 MeV above the equilibrium minimum. The red dots in each panel indicate the points on the dynamical (least-action) path for α emission, and the insets display the corresponding intrinsic nucleon densities along the path, starting from the equilibrium deformation up to the scission point. A clear formation of cluster of nucleons can be observed in the last density plots, and we have verified that the integrated density of this cluster is four nucleons. The first part of the action is then calculated from the inner point to the scission one and leads to a value of $S_S = 7.07$. Beyond the scission point and up to the outer point, the dynamics between the two fragments is determined by the Coulomb repulsion [9] and we have calculated the value of $S_C = 9.46$ leading to a total of $S = 16.53$ and a corresponding alpha half-live is $T_\alpha = 0.6\,\mu$s, to be compared with the experimental value of $0.3\,\mu$s.

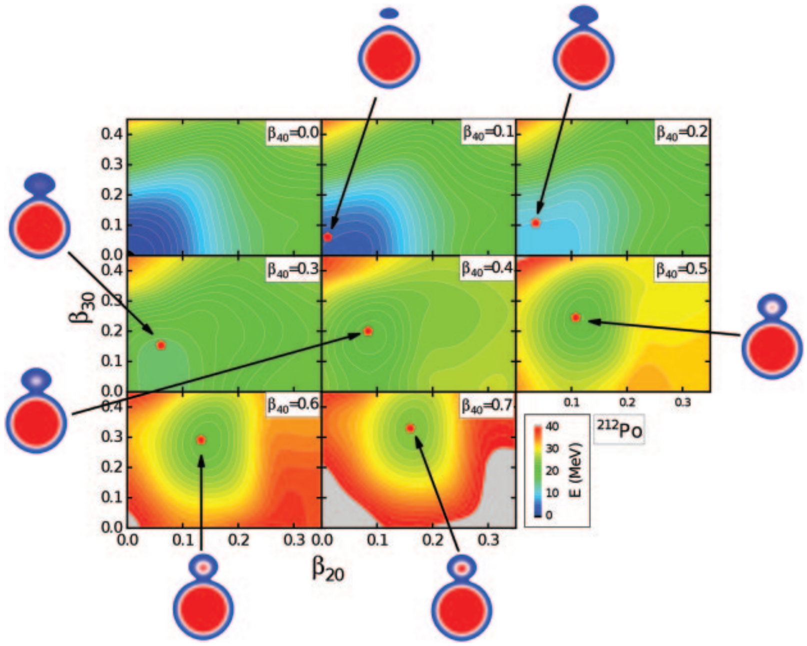

Fig. 1. – Deformation energy surface of ^{212}Po in the quadrupole-octupole axially-symmetric plane, for selected values of the hexadecapole deformation β_{40}. Red circles indicate the points on the dynamical (least-action) path for α emission. The insets display the intrinsic nucleon densities at selected points on the dynamical path. Figure taken from [37].

Similar calculations were performed on ^{224}Ra, leading to a scission point for α decay located at $(\beta_{20}, \beta_{30}, \beta_{40}) \simeq (0.15, 0.31, 0.68)$. Up to the scission point, the contribution to the action is of $S_S = 9.96$ and the Coulomb part from scission to outer point $S_C = 20.50$. The predicted α half-life then reaches 9.5 days, in qualitative agreement with the experimental value of 3.6 days.

Two α decay

The idea of emitting two α particles is not new. Already some predictions [38], and detection [39] of 2α particles during fission process have been made. As already mentioned, the case of a ^{8}Be cluster emission [7] has also been studied, leading to a 2α state because of the resonant nature of ^{8}Be ($Q_\alpha = 92\,\text{keV}$). This particular decay has been discussed in ref. [5], and recently a possible experimental investigation has been considered in ref. [6]. These studies showed that the corresponding half-life would be approximated by the one of ^{8}Be cluster emission. As a consequence, the half-live reaches very high values of the order of $\log\, T\,[s] \simeq 50$ to 100, typically. However, here, we propose a different decay type corresponding to a spontaneous emission of two α particles.

The microscopic self-consistent framework used in this study can provide complementary insight on the direct 2α decay process. In particular, in the following we show that two α particles can be emitted back to back, in a symmetric way, rather than in a ^{8}Be-like mode with a significantly reduced half-life compared to those of ^{8}Be cluster emission discussed above. For a broader study of the possible candidates for 2α decay, see [37].

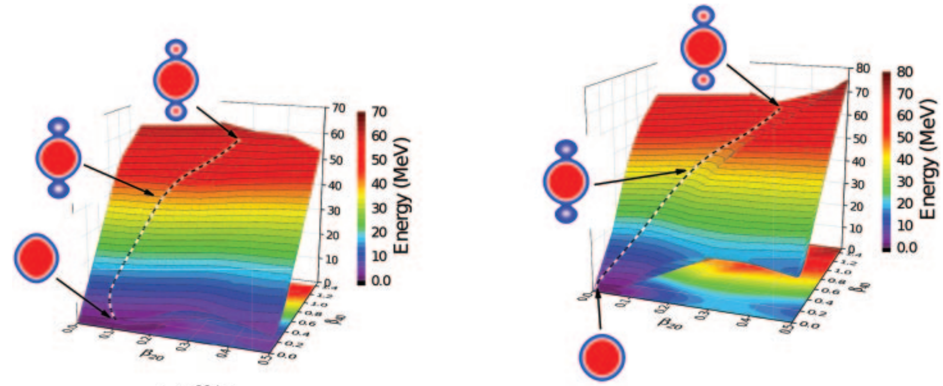

(a) ^{224}Ra.

(b) ^{212}Po.

Fig. 2. – Reflection symmetric deformation energy surface of ^{224}Ra and ^{212}Po in the quadrupole-hexadecapole axially-symmetric plane. The black and white dashed curve denotes the dynamical (least-action) path for 2α emission from equilibrium deformation to scission, and the insets display the intrinsic nucleon densities for three selected points on the path. Figures taken from [37].

As previously mentioned, the 2α decay is described here as a symmetric process and hence involving only quadrupole and hexadecapole collective coordinates. Figure 2(a) displays the axially-symmetric energy surface of ^{224}Ra, as a function of the quadrupole and hexadecapole intrinsic deformations. The dynamic path for 2α emission starting from the equilibrium deformation and up to the scission point located at $(\beta_{20}, \beta_{40}) \simeq (0.28, 1.30)$, is traced by the dashed curve. We found a first contribution to the action eq. (1) of $S_S = 16$. From the scission point to the outer one, only the Coulomb interaction is considered again. This yields a scission to 2α emission action of $S_C = 23.89$. Combining both these paths, a 2α half-life of $\log(T_{2\alpha}[s]) = 14.24$ is obtained, much shorter than the ^{8}Be-like emission half-life $\log(T_{2\alpha}[s]) = 27.87$, calculated using the semi-empirical model for cluster decay of ref. [40]. Similar results of symmetric 2α decay half-life (to within one order of magnitude) have been obtained with few other standard relativistic energy density functionals. It could, therefore, be interesting to reconsider the cluster detection experiment for this nucleus, aiming to detect two α clusters in coincidence at 180 degree. The insets in fig. 2(a) display the intrinsic nucleon densities for three selected points on the 2α emission dynamic path. The 2α configuration is clearly visible for the configuration at the scission point.

Similar calculations can be performed for other nuclei. The case of ^{212}Po is for instance depicted in fig. 2(b) with a scission point located at $(\beta_{20}, \beta_{40}) \simeq (0.32, 1.46)$. The dynamical path up to the scission point exhibits quite a similar pattern as in the case of ^{224}Ra with a contribution to the action of $S_S = 15.56$. The Coulomb contribution reads $S_C = 15.56$ leading to a final half-life of $\log(T_{2\alpha}[s]) = 18.36$ for 2α half-life of ^{212}Po. This result can be compared to the ^{8}Be decay channel $\log(T_{2\alpha}[s]) = 38.82$ [40].

Conclusion

In summary, the method of self-consistent mean-field based on the relativistic DD-PC1 energy density functional and separable pairing interaction has been used to analyse single α and double α emission processes in ^{212}Po and ^{224}Ra. It has been shown that these processes are characterized by half-lives that can differ by orders of magnitude, from 10^{15} s (2α emission) to days or microseconds (α emission). In the case of the predicted 2α decay process, where two α particles are emitted back to back in opposite directions, predicted half-lives are of the order of those detected for already observed cluster decay modes (from ^{14}C to ^{34}Si). Compared to the ^{8}Be decay channel results, this study leads to half-lives that are many order of magnitude shorter, leading to possible experimental investigation using α detectors in coincidence at 180 degrees.

* * *

This work has been supported in part by the QuantiXLie Centre of Excellence, a project co-financed by the Croatian Government and European Union through the European Regional Development Fund - the Competitiveness and Cohesion Operational Programme (KK.01.1.1.01.0004) and the Croatian Science Foundation under the project Uncertainty quantification within the nuclear energy density framework (IP-2018-01-5987). JZ acknowledges support by the NSFC under Grants No. 12005107 and No. 11790325. J-PE, EK and FM thank R. Lasseri for fruitful discussions.

REFERENCES

[1] Delion D. S., *Lect. Notes Phys.*, **819** (2010) 1.
[2] Rose H. J. and Jones G. A., *Nature*, **307** (1984) 245.
[3] Giovinazzo J. *et al.*, *Phys. Rev. Lett.*, **89** (2002) 102501.
[4] Pfützner M. *et al.*, *Eur. Phys. J. A*, **14** (2002) 279.
[5] Poenaru D. N. and Ivascu M., *J. Phys. Lett.*, **46** (1985) 591.
[6] Tretyak V. I., arXiv:2102.12005 [nucl-ex] (2021).
[7] Poenaru D. N. and Greiner W., *Lect. Notes Phys.*, **818** (2010) 1.
[8] Gupta R. K., *Lect. Notes Phys.*, **818** (2010) 223.
[9] Warda M. and Robledo L. M., *Phys. Rev. C*, **84** (2011) 044608.
[10] Warda M., Zdeb A. and Robledo L. M., *Phys. Rev. C*, **98** (2018) 041602(R).
[11] Vretenar D., Afanasjev A. V., Lalazissis G. A. and Ring P., *Phys. Rep.*, **409** (2005) 101.
[12] Marević P., Ebran J. P., Khan E., Nikšić T. and Vretenar D., *Phys. Rev. C*, **97** (2018) 024334.
[13] Marević P., Ebran J. P., Khan E., Nikšić T. and Vretenar D., *Phys. Rev. C*, **99** (2019) 034317.
[14] Zhao J., Lu B.-N., Nikšić T. and Vretenar D., *Phys. Rev. C*, **92** (2015) 064315.
[15] Zhao J., Lu B.-N., Nikšić T., Vretenar D. and Zhou S.-G., *Phys. Rev. C*, **93** (2016) 044315.
[16] Tao H., Zhao J., Li Z. P., Nikšić T. and Vretenar D., *Phys. Rev. C*, **96** (2017) 024319.
[17] Zhao J., Nikšić T., Vretenar D. and Zhou S.-G., *Phys. Rev. C*, **99** (2019) 014618.
[18] Zhao J., Xiang J., Li Z.-P., Nikšić T., Vretenar D. and Zhou S.-G., *Phys. Rev. C*, **99** (2019) 054613.
[19] Mercier F., Zhao J., Lasseri R.-D., Ebran J. P., Khan E., Nikšić T. and Vretenar D., *Phys. Rev. C*, **102** (2020) 011301(R).

[20] Ebran J. P., Khan E., Lasseri R. D. and Vretenar D., *Phys. Rev. C*, **97** (2018) 061301(R).
[21] Ebran J. P., Khan E. and Lasseri R. D., *J. Phys. G: Nucl. Part. Phys.*, **48** (2021) 025106.
[22] Meng J., *Relativistic Density Functional for Nuclear Structure* (World Scientific) 2016.
[23] Ebran J. P., in *Energy Density Functional Methods for Atomic Nuclei* (IOP Publishing) 2019.
[24] Brack M., Damgaard J., Jensen A. S., Pauli H. C., Strutinsky V. M. and Wong C. Y., *Rev. Mod. Phys.*, **44** (1972) 320.
[25] Ledergerber T. and Pauli H.-C., *Nucl. Phys. A*, **207** (1973) 1.
[26] Baran A., *Phys. Lett. B*, **76** (1978) 8.
[27] Baran A., Pomorski K., Lukasiak A. and Sobiczewski A., *Nucl. Phys. A*, **361** (1981) 83.
[28] Sadhukhan J., Mazurek K., Baran A., Dobaczewski J., Nazarewicz W. and Sheikh J. A., *Phys. Rev. C*, **88** (2013) 064314.
[29] Sadhukhan J., Dobaczewski J., Nazarewicz W., Sheikh J. A. and Baran A., *Phys. Rev. C*, **90** (2014) 061304(R).
[30] Hill D. L. and Wheeler J. A., *Phys. Rev.*, **89** (1953) 1102.
[31] Staszczak A., Baran A. and Nazarewicz W., *Phys. Rev. C*, **87** (2013) 024320.
[32] Baran A., Staszczak A., Dobaczewski J. and Nazarewicz W., *Int. J. Mod. Phys. E*, **16** (2007) 443.
[33] Lu B.-N., Zhao J., Zhao E.-G. and Zhou S.-G., *Phys. Rev. C*, **89** (2014) 014323.
[34] Nikšić T., Vretenar D. and Ring P., *Phys. Rev. C*, **78** (2008) 034318.
[35] Tian Y., Ma Z. Y. and Ring P., *Phys. Lett. B*, **676** (2009) 44.
[36] Teeti S. and Afanasjev A. V., *Phys. Rev. C*, **103** (2021) 034310.
[37] Mercier F., Zhao J., Ebran J.-P., Khan E., Nikšić T. and Vretenar D., *Phys. Rev. Lett.*, **127** (2021) 012501.
[38] Poenaru D. N. *et al.*, *Phys. Rev. C*, **59** (1999) 3457.
[39] Gönnewein F., Mutterer M. and Kopatch Y., *Europhys. News*, **36** (2005) 11.
[40] Poenaru D. N. *et al.*, *Phys. Rev. C*, **65** (2002) 054308.